

# An Estimation of Areal Distribution of Evapotranspiration over Khentii Region Using a Combination of Satellite Data and a Heat Budget Model

Matsushima, D.<sup>1</sup>, Y. Matsuura<sup>1</sup>, I. Byambakhuu<sup>2</sup>, Ts. Adyasuren<sup>2</sup>

<sup>1</sup> Department of Geophysics, Tohoku University, Japan, <sup>2</sup> ECO Asia, Mongolia

Keywords: evapotranspiration, satellite, remote sensing, heat budget model

## Introduction

This study aims to estimate spatial distribution of evapotranspiration over a typical steppe region in Mongolia. A precise estimate of temporal and spatial distribution of evapotranspiration over the region is significant to determine local and regional water budget in and around the region. The subject area in this study is a steppe divided by a square which is in the range of latitude between 46-48deg N and longitude 108-111deg E, where is almost in the Kherlen River watershed. As for vegetation distribution, typical steppe is dominant in this squared area including a little forest-steppe in northern part and dry-steppe in southern part. The final goal of this study is to establish a scheme to estimate spatial and temporal distribution of surface heat budget and evapotranspiration using routine satellite data and a heat budget model. Some preliminary results of remote sensing and estimation of evapotranspiration are shown in parallel at this time, and they will be merged into a continuous scheme in the near future.

## Algorithm

A schematic illustration of algorithm of combination of remote sensing and surface heat budget model for estimating spatial distribution of evapotranspiration in this study is shown in Fig. 1. The remote sensing consists of three classifications, which are satellite data, airborne observation, and ground-based observation. The

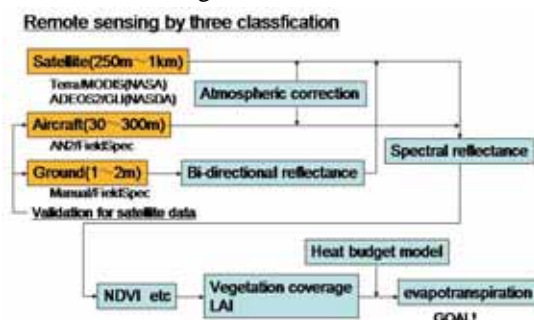


Fig.1 Schematic of estimation algorithm.

satellite data is used for spatial distribution maps of various variables, such as surface brightness temperature, normalized difference vegetation index (NDVI), and etc. The airborne and the ground-based observations are used for validation of satellite data. Measurement conditions of satellite data are so distributed that the NDVI and other products of different conditions are not always consistent, and that may make error in estimating leaf area index (LAI), and other physical parameters. Those parameters are finally applied to the surface heat budget model to estimate spatial distribution of evapotranspiration over a steppe in the subject region.

## Data

### Remote sensing data

Two archives of satellite data in the subject area are used in this study. One is NASA-EOS/MODIS L1B data, which is an archive of 36 channels of visible and near-infrared reflectance, and thermal-infrared radiance. Spatial resolution is about 1km, and the frequency is one or two times in one daytime. The data in need are easily collected from the MODIS web server. In this study, the MODIS data are used for estimating LAI, surface temperature, and other physical product, which optimize the parameters in the surface heat budget model. The other one is geostational satellite GOES-9 data, which consists of visible reflectance and thermal-infrared temperature every one hour. The GOES-9 data are also easily collected from an archive in Kochi University by internet. Spatial resolution is originally 1.25km for visible data, and 4km for thermal-infrared data, but the resolution of archived data is 0.05deg (about 5km). The GOES-9 data are used for estimating incoming solar radiation on the earth surface using an algorithm which is described in later section.

Airborne observations were carried out

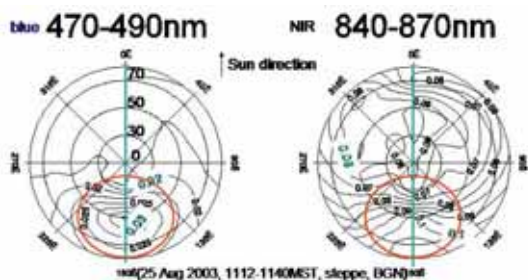


Fig.2 An example of bi- directional reflectance which depends on measuring angle.

in the intensive observation periods between May and October 2003. A FieldSpec, visible and near-infrared spectro-radiometer, was installed on an aircraft AN-2. The spectro-radiometer viewed steppe and forest surface in nadir angle out of the aircraft bottom window with a field-of-view of 18 deg. The flight path was a route connecting Ulaanbaatar and observing stations. The FieldSpec was also used in ground-based observations, which carried out bi-directional reflectance spectrometry over a steppe, a forest canopy, some water surfaces.

*Meteorological data*

Some basic meteorological data, including radiation and soil temperature and moisture, are acquired in four automatic weather stations (AWSs) in the subject area. They are continuously measured and archived every 10 minutes from March 2003. In this study, 1-hour average data of them are used as input variables and validation variable in the surface heat budget model.

**Bidirectional Characteristics of NDVI**

*Ground-based data*

Figure 2 illustrates an example of bi-directional reflectance distribution of a visible band. The reflectance tends to increase as the nadir viewing angle increases, and the reflectance pattern is symmetrical if the surface is almost

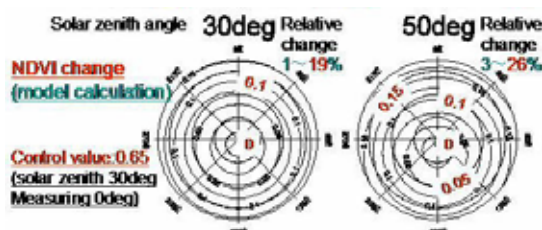


Fig.3 NDVI difference from the control value, which depends on solar altitude and measuring angle which is indicated by the distance from the circle center.

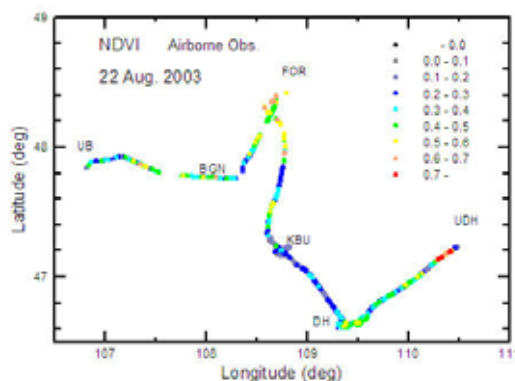


Fig.4 NDVI estimated from airborne spectrometry.

homogeneous. These characteristics of other visible and near-infrared bands are almost the same. Remote sensing indices, such as NDVI, are influenced by these reflectance characteristics. Figure 3 shows the change of NDVI depends on solar altitude and the measuring angle. The anomaly from the value of standard (solar angle = 30deg, measuring angle = 0deg) is as large as 30% of the standard value.

*Airborne data*

Figure 4 shows a result of NDVI by an airborne observation on 22 Aug. 2003. These NDVI values are compared to a satellite data obtained on the same day, which was almost synchronized with the airborne observation. Figure 5 shows the difference between the two ways of estimates, which reveals overestimation of satellite NDVI when the absolute values were small. This is consistent with the results of the ground-based observation, because the measuring angles of satellite is around 50-60deg from nadir while that of the airborne observation is almost nadir.

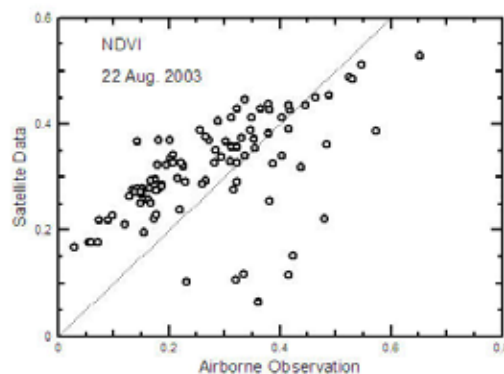


Fig.5 Comparison of NDVI estimation by airborne observation and satellite data.

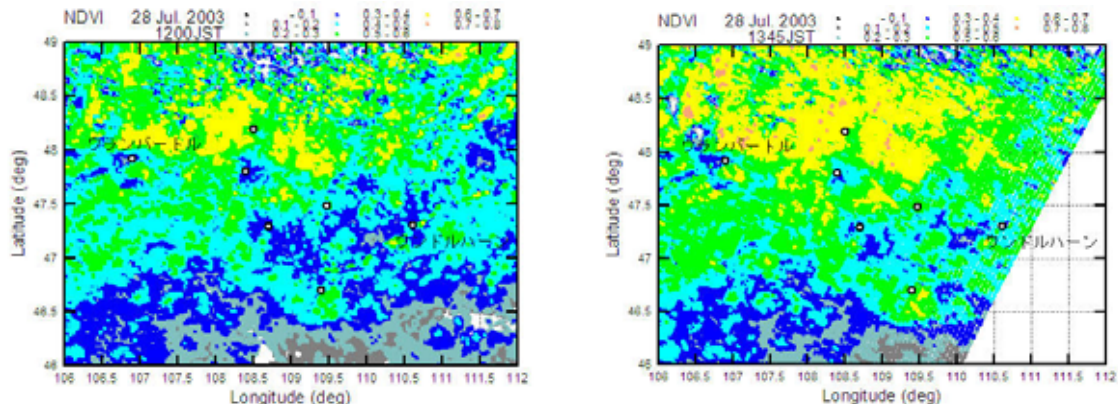


Fig.6 Difference of NDVI estimation between two satellite images of 1200h and 1345h 28 Jul. 2003.

*Satellite data*

Figure 6 illustrates maps of NDVI distribution observed by the same satellite but observing times were a bit different. The overall NDVI values are remarkably different though the observation interval was only less than two hours. Parameters regarding the observations were almost the same, but only measuring angles were different, which were 50deg and 60deg. Even a little difference of measuring angles larger than 50deg may result crucial difference in reflectance and further NDVI.

*Estimation of LAI*

LAI can be roughly estimated by a linear empirical equation of NDVI obtained by the least squares method. The dependence of NDVI on the solar altitude and the measuring angle also affects the estimation of LAI (not shown in figure).

**Surface Solar Radiation by Satellite**

The geostational satellite GOES-9, which views East Asia and Oceania, obtains visible and infrared images every hour. Kawamura et al. (1999) developed an algorithm for estimating incoming solar radiation at surface. Spatial distribution of solar radiation over the subject area is estimated every hour using this algorithm with parameters of which being optimized so as to minimize difference between the estimates and observed values at the AWS stations. An example of results is shown in Fig. 7.

**Surface Heat Budget Model**

*Prognostic equation*

The heat budget model used in this study is based on the force-restore method for forecasting earth surface temperature and the bulk

formulation to estimate sensible and latent heat fluxes (Matsushima and Kondo, 1995). A summarized form of the equation is given as:

$$\frac{d}{dt} \begin{pmatrix} T_g \\ T_c \end{pmatrix} = A \begin{pmatrix} T_g \\ T_c \end{pmatrix} + B(S, L, T_a, q, U)^t, \quad (1)$$

where  $T_g$  and  $T_c$  are surface temperature of bare soil and vegetation canopy,  $S$  and  $L$  are incoming solar and longwave radiation,  $T_a$  is the air temperature,  $q$  the specific humidity, and  $U$  the wind speed. Parameter matrices  $A$  and  $B$  include albedo, the bulk transfer coefficients, evaporation efficiency, and etc. Finally, the surface brightness temperature  $T_r$  is calculated from  $T_g$  and  $T_c$ .

*Optimizing surface parameters*

Parameters regarding land surface processes should be optimized to have reasonable estimation of evapotranspiration. In this study, the daily average of the bulk transfer coefficient for sensible heat  $C_H$ , the slope of the bulk coefficient regarding wind speed  $b$ , and the evaporation efficiency are optimized both for bare soil and canopy, while the other parameters such as albedo are given. The optimizing is achieved by minimizing the difference between estimation of

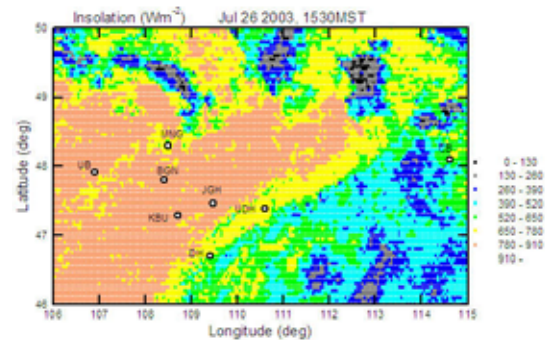


Fig.7 An example of solar insolation using GOES-9 data at 1530h 26 Jul. 2003.

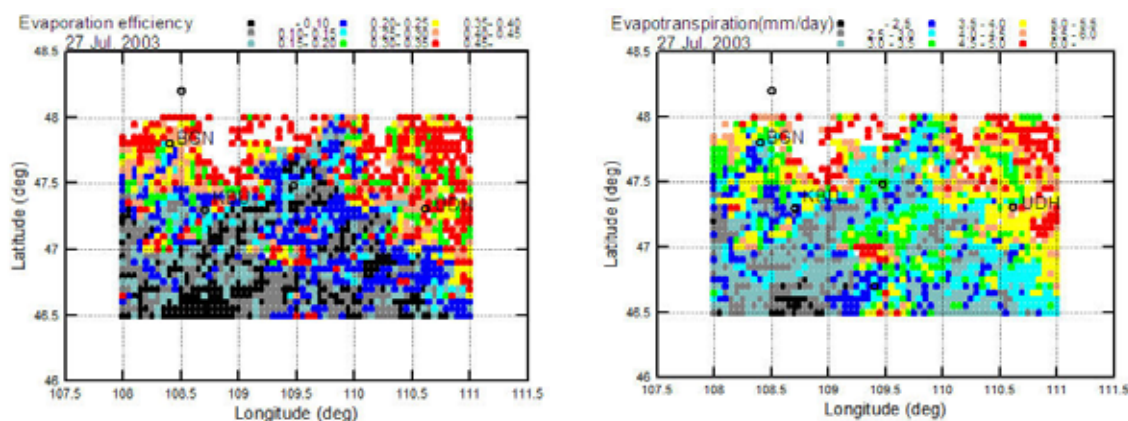


Fig.8 (left) Evaporation efficiency and (right) daily average of evapotranspiration in the subject area on 27 Jul 2003.

$T_r$  and the satellite brightness temperature. More than six samples of observed surface temperature are needed for optimization because there are six parameters which should be optimized. In this study, the parameters at the AWS stations are determined using temporal change of surface infrared temperature in daytime every day. Other than the AWS stations, daily values of the surface parameters are determined at every GOES-9 grid, and using the spatial change of satellite infrared temperature, because the satellite data is usually obtained only once or twice in a daytime.

### Estimation of Spatial Distribution of Evapotranspiration

Figure 8 shows the spatial distribution of evaporation efficiency and the daily average of evapotranspiration on 27 Jul. 2003. These figures roughly illustrate surface moisture conditions in 5km resolution. To validate these results, diurnal changes of surface heat flux at Kherlen-Bayan Ulaan (KBU) are illustrated in Fig. 9. The daytime surface temperature is almost reproduced, while heat fluxes are not so sufficiently reproduced except the net radiation. Several reasons should be taken into account. One of which is an overestimation of evaporation efficiency. Actually, the monthly amount of evapotranspiration of July 2003 at KBU is slightly more than precipitation. Second reason is observed sensible and latent heat fluxes are underestimated. The sum of the heat fluxes other than net radiation is less than the net radiation. That is because the observed values of sensible and latent heat fluxes are less than the calculation. However, the Bowen ratio of both calculation and observation are almost the same.

### Summary and Future Issues

Some preliminary results of the bi-directional reflectance characteristics over steppe surface are shown. On the other hand, using both the satellite temperature and the heat budget model, a spatial distribution of evapotranspiration is calculated, and validated with the ground observation, though the overestimation is found in evapotranspiration. Future issue is to merge the two studies and accomplish the whole scheme of estimating evapotranspiration.

### Acknowledgments

This study is carried out as a study of the JST-CREST/RAISE project. Dr. Saandar and MIAT Co., Ltd. totally supported the airborne observations.

### References

- Kawamura, H. et al., Estimation of insolation over the Pacific Ocean off the Sanriku Coast, *J. Oceanography*, **54**, 457-464, 1998.
- Matsushima, D. and J. Kondo, An estimation of the bulk transfer coefficients for a bare soil surface using a linear model, *J. Applied Meteorology*, **34**, 927-940, 1995.

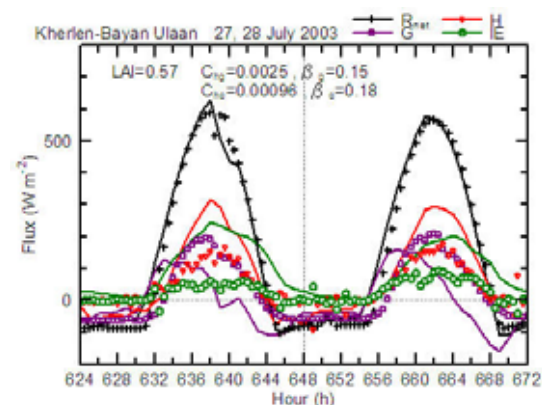


Fig.9 An example of diurnal change of surface heat budget at KBU on 27 and 28 Jul. 2003.